Journal of Vibration and Acoustics

Technical Briefs

Dynamic Characteristics of a One-Unit Ball-Rod-Spring Balancer

Ming-Cheng Wang
Graduate Student

Chung-Jen Lu[1]
Associate Professor
e-mail: cjlu@ntu.edu.tw

Department of Mechanical Engineering,
National Taiwan University,
No. 1 Roosevelt Rd. Sec. 4,
Taipei 10617, Taiwan,
Republic of China

The traditional ball-type automatic balancer consisting of several balls moving on a circular orbit is widely used in the optical disk drive industry for vibration reduction. Under proper working conditions, the balls can counterbalance the imbalance of a disk by positioning to appropriate angles relative to the mass center of the disk. This particular equilibrium position is referred to as the perfect balancing position. The proper working conditions are closely related to the stability of the perfect balancing position, which, in turn, depends on the parameters of the system, such as rotational speed, imbalance ratio, and damping ratios. To achieve perfect balancing, the system parameters must lie in the stable region of the perfect balancing position in the parameter space. An automatic balancer with a wider stable region can tolerate a larger amount of variations in the system parameters and hence is more robust. In this study, we propose a modified ball-type balancer composed of several ball-rod-spring units. In each unit, the ball can slide along the rod while the rod rotates freely about the spindle. The ball's displacement along the rod is restrained by a radial spring. The additional degree of freedom in the radial direction could broaden the stable region of the perfect balancing position. To understand the fundamental properties of the modified balancer, we studied the dynamic characteristics of a modified balancer with one ball-rod-spring unit. Specifically, we built a theoretical model for an optical disk drive packed with the modified balancer, and investigated how equilibrium positions and the associated stability are related to primary system parameters and the effects of the stiffness of the radial spring on the stable region of the perfect balancing position. Numerical results indicate that the ball-rod-spring balancer may possess a larger stable region of the perfect balancing position compared to the traditional fixed-orbit balancer. [DOI: 10.1115/1.2748462]

1 Introduction

Ball-type automatic balancers can effectively reduce the imbalance vibrations of the optical disk drives and have been investigated by many researchers [1–11]. The most popular ball-type automatic balancer used in the optical disk drive industry is composed of several balls moving along a fixed circular orbit. For the convenience of discussion, this kind of balancer is referred to as the fixed-orbit balancer. Under proper working conditions, the balls will move to specific equilibrium positions where the imbalance vibrations are totally suppressed. These equilibrium positions are called the perfect balancing positions, and their stability characteristics dictate the proper working conditions. The primary system parameters that govern the stability of the perfect balancing position are the ratio of the disk speed to the natural frequency of the system, the ratio of the imbalance of the balancer to that of the disk, and the respective damping of the suspension and the balancer [5–8,10,11]. The stability of the perfect balancing position of the fixed-orbit balancer with one ball [4,8,11] and two balls [5–7,10] have been examined extensively, and the corresponding stable regions on the parameter plane were identified. In order to suppress the imbalance vibrations, the system parameters under working conditions must lie in the stable region of the perfect balancing position. A large stable region indicates more tolerance to the variations of the system parameters and, hence, a robust performance. An interesting question arises if the stable region can be broadened by relaxing the constraint that the balls can only move along a fixed circular orbit. To answer this question, we propose a modified balancer in which an extra degree of freedom is introduced to the balls. The modified balancer is composed of several ball-rod-spring units. Each unit consists of a ball sliding along a rod that rotates about the spindle. The motion of the ball along the rod is restrained by a linear spring. The results of preliminary numerical analysis indicate that the ball-rod-spring balancer possesses lower critical speed compared to the fixed-orbit balancer [12]. The aim of this paper is to systematically investigate the dynamic characteristics of the ball-rod-spring balancer.

It is well known that at least two balls are required to automatically counter-balance arbitrary amount of imbalance. For an automatic balancer with two balls, the equilibrium positions of the balls can be classified into three different types: (i) the two balls stick together; (ii) the two balls stay respectively on the two ends of a diameter; or (iii) the two balls separate at a specific angle. For each type of equilibrium position, the two balls can be replaced by a single ball of proper mass. In this case, the two-ball system is equivalent to a one-ball system [4,8,11]. As a result, the amplitude of vibration of the two-ball system can be determined from the formula of the one-ball system by substituting a proper value for the imbalance ratio. Moreover, it can be shown that the equilibrium position of a two-ball system is unstable if the corresponding

[1]Corresponding author.

Contributed by the Technical Committee on Vibration and Sound of ASME for publication in the JOURNAL OF VIBRATION AND ACOUSTICS. Manuscript received: November 14, 2005; final manuscript received April 16, 2007. Assoc. Editor: I.Y. (Steve) Shen.

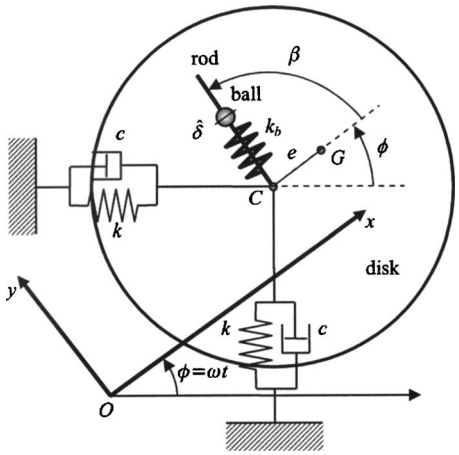

Fig. 1 Schematic diagram of the balancer-rotor system and rotating reference frame

one-ball system is unstable. Therefore, the analysis of a one-ball system not only greatly reduces the algebraic work but also provides valuable insight into the properties of the two-ball system. To further understand the fundamental dynamic characteristics of the modified balancer without heavy algebraic work involved, we studied a modified balancer with one ball-rod-spring unit. This paper describes the results of the study. It first shows the dynamic model that we developed for an optical disk drive equipped with the modified balancer. Then the nonlinear governing equations are derived from the Lagrange's equations with respect to a corotating coordinate system. After that, the formulas of the equilibrium positions are presented and the stable region of each equilibrium position in the parameter space is identified numerically. Finally, the stable region of the perfect balancing position of the ball-rod-spring balancer is compared to that of the traditional fixed-orbit balancer.

2 Mathematical Model

Figure 1 shows the schematic of the ball-rod-spring balancer and the reference frame. Each ball-rod-spring unit consists of a ball sliding along a rod that rotates about the geometric center C of the disk. The motion of the ball along the rod is restrained by a radial spring with stiffness k_b and unstretched length $\hat{a}$. The disk with mass m_d rotates with a constant angular velocity ω. The mass center G of the disk is located at a distance e from the geometric center C. The suspension system is isotropic and can be characterized by equivalent linear springs with stiffness k and viscous dampers with damping constant c. When the disk is at rest, its geometric center C coincides with the origin O and the suspension springs are undeformed. The xy reference frame rotating with the same angular velocity ω as the disk is used to formulate the problem because the equations of motion expressed in this frame are autonomous. When the disk is rotating, its geometric center C undergoes a translational motion in the xy frame. The position of C is indicated by the coordinates $(\hat{x},\hat{y})$. The position of the ball is given by the distance $\hat{\delta}$ from C and the angle β relative to the mass center G.

The equations of motion are derived from Lagrange's equations and can be expressed in dimensionless form as

$$x'' + \mu_b\{[\delta'' - \delta(\beta' + \Omega)^2]\cos\beta - [\delta\beta'' + 2\delta'(\beta' + \Omega)]\sin\beta\} - \frac{\mu_b\Omega^2}{\eta} + 2\varsigma x' - 2\Omega y' + (1-\Omega^2)x - 2\varsigma\Omega y = 0 \quad (1)$$

$$y'' + \mu_b\{[\delta'' - \delta(\beta' + \Omega)^2]\sin\beta + [\delta\beta'' + 2\delta'(\beta' + \Omega)]\cos\beta\} + 2\varsigma y' + 2\Omega x' + (1-\Omega^2)y + 2\varsigma\Omega x = 0 \quad (2)$$

$$\mu_b\delta[(y'' + 2\Omega x' - \Omega^2 y)\cos\beta - (x'' - 2\Omega y' - \Omega^2 x)\sin\beta + \delta\beta'' + 2\delta'(\beta' + \Omega)] + 2\varsigma_b\mu_b\delta^2\beta' = 0 \quad (3)$$

$$\mu_b[(x'' - 2\Omega y' - \Omega^2 x)\cos\beta + (y'' + 2\Omega x' - \Omega^2 y)\sin\beta - \delta(\beta' + \Omega)^2 + \delta''] + 2\varsigma_b\mu_b\delta' + \mu_b f^2(\delta - 1) + \mu_b\Omega^2 = 0 \quad (4)$$

where $(\,)'$ indicates differentiation with respect to $\tau = \omega_n t$ and

$$\lambda = \frac{k_b\hat{a}}{k_b - m_b\omega^2}, \quad x = \frac{\hat{x}}{\lambda}, \quad y = \frac{\hat{y}}{\lambda}, \quad \delta = \frac{\hat{\delta}}{\lambda}$$

$$a = \frac{\hat{a}}{\lambda}, \quad \Lambda = \frac{e}{\lambda}, \quad c = 2M\varsigma\omega_n, \quad c_b = 2m_b\varsigma_b\omega_n$$

$$\omega_n = \sqrt{\frac{k}{M}}, \quad \omega_b = \sqrt{\frac{k_b}{m_b}}, \quad \mu_b = \frac{m_b}{M}$$

$$\eta = \frac{m_b\lambda}{m_d e}, \quad \Omega = \frac{\omega}{\omega_n}, \quad f = \frac{\omega_b}{\omega_n} \quad (5)$$

in which M is the total mass of the system. It is worth noting that λ is the steady-state length of the radial spring k_b when the system is perfectly balanced, η the ratio of the imbalance of the balancer to that of the disk at steady state, Ω the ratio of the rotational speed of the disk to the natural frequency of the system.

3 Equilibrium Position

The first step in analyzing a nonlinear system is to identify the equilibrium positions. The equilibrium positions, denoted by $\tilde{x}$, $\tilde{y}$, $\tilde{\beta}$, and, $\tilde{\delta}$ can be deduced from Eqs. (1)–(4) by suppressing the time derivatives and solving the resulting algebraic equations,

$$\begin{cases} (1-\Omega^2)\tilde{x} - 2\varsigma\Omega\tilde{y} - \mu_b\tilde{\delta}\Omega^2\cos\tilde{\beta} - \dfrac{\mu_b\Omega^2}{\eta} = 0 \\ 2\varsigma\Omega\tilde{x} + (1-\Omega^2)\tilde{y} - \mu_b\tilde{\delta}\Omega^2\sin\tilde{\beta} = 0 \\ \mu_b\tilde{\delta}\Omega^2(\tilde{x}\sin\tilde{\beta} - \tilde{y}\cos\tilde{\beta}) = 0 \\ -\mu_b\Omega^2(\tilde{x}\cos\tilde{\beta} + \tilde{y}\sin\tilde{\beta}) + \mu_b(f^2 - \Omega^2)(\tilde{\delta} - 1) = 0 \end{cases} \quad (6)$$

To solve Eqs. (6), we introduce the polar coordinates

$$\tilde{x} = \tilde{r}\cos\tilde{\theta}, \quad \tilde{y} = \tilde{r}\sin\tilde{\theta}$$

and rewrite Eqs. (6) as

$$\begin{cases} (1-\Omega^2)\tilde{r}\cos\tilde{\theta} - 2\varsigma\Omega\tilde{r}\sin\tilde{\theta} - \mu_b\tilde{\delta}\Omega^2\cos\tilde{\beta} - \dfrac{\mu_b\Omega^2}{\eta} = 0 \\ 2\varsigma\Omega\tilde{r}\cos\tilde{\theta} + (1-\Omega^2)\tilde{r}\sin\tilde{\theta} - \mu_b\tilde{\delta}\Omega^2\sin\tilde{\beta} = 0 \\ \mu_b\tilde{\delta}\Omega^2\tilde{r}\sin(\tilde{\beta} - \tilde{\theta}) = 0 \\ -\mu_b\Omega^2\tilde{r}\cos(\tilde{\beta} - \tilde{\theta}) + \mu_b(f^2 - \Omega^2)(\tilde{\delta} - 1) = 0 \end{cases} \quad (7)$$

Equation (7.3) admits three solutions: $\tilde{r}=0$, $\tilde{\beta}=\tilde{\theta}$, and $\tilde{\beta}=\tilde{\theta}+\pi$. Equilibrium positions associated with these three cases of solutions and the conditions under which they exist are discussed separately below.

(i) $\tilde{r}=0$. In this case, the system is perfectly balanced and has no residual vibration at steady state. Substituting $\tilde{r}=0$ into Eqs. (7) yields

$$\begin{cases} -\mu_b\tilde{\delta}\Omega^2\cos\tilde{\beta} = \dfrac{\mu_b\Omega^2}{\eta} \\ \mu_b\tilde{\delta}\Omega^2\sin\tilde{\beta} = 0 \\ \mu_b(f^2 - \Omega^2)(\tilde{\delta} - 1) = 0 \end{cases} \quad (8)$$

whence

$$\tilde{\delta} = \eta = 1 \quad \text{and} \quad \tilde{\beta} = \pi$$

The above results indicate that perfect balancing is possible only if the balancer has the same imbalance as the disk and the ball is located on the opposite side of the diameter passing through the geometric center of the disk at steady state.

(ii) $\tilde{\beta} = \tilde{\theta}$. Substituting $\tilde{\beta} = \tilde{\theta}$ into Eqs. (7.1) and (7.2) gives, after some rearrangements,

$$\begin{cases} -[(\Omega^2 - 1)\tilde{r} + \mu_b \tilde{\delta}\Omega^2] = \dfrac{\mu_b \Omega^2 \cos\tilde{\theta}}{\eta} \\ -2\zeta\Omega r = \dfrac{\mu_b \Omega^2 \sin\tilde{\theta}}{\eta} \end{cases}$$

By squaring and adding, we obtain the two possible solutions as

$$\left.\begin{matrix} \tilde{r}_{11} \\ \tilde{r}_{12} \end{matrix}\right\} = R_{NS}(-\eta \cdot p \pm \sqrt{D_{NS}}) \tag{9}$$

where

$$R_{NS} = \frac{\Omega^2 \mu_b (f^2 - \Omega^2)}{\eta(p^2 + q^2)} \quad \text{and} \quad D_{NS} = p^2 + q^2 - \eta^2 q^2 \tag{10}$$

in which p and q are functions of Ω as defined below

$$p = (f^2 - \Omega^2)(\Omega^2 - 1) + \Omega^4 \mu_b \quad \text{and} \quad q = 2\varsigma\Omega(f^2 - \Omega^2) \tag{11}$$

The corresponding $\tilde{\theta}$ and $\tilde{\delta}$ are determined by

$$\tilde{\theta} = \tan^{-1} \frac{2\varsigma\Omega \cdot \tilde{r}}{(\Omega^2 - 1) \cdot \tilde{r} + \mu_b \Omega^2 \tilde{\delta}} \tag{12}$$

$$\tilde{\delta} = 1 + \frac{\Omega^2 \tilde{r}}{f^2 - \Omega^2} \tag{13}$$

Note that $\tilde{r}$ and $\tilde{\delta}$ should be real and non-negative. Since $\tilde{\delta} > 1$ if $\tilde{r} \geqslant 0$, we only need to consider the conditions under which $\tilde{r}$ is non-negative. The results are summarized as follows:

$$\tilde{r}_{11} \geqslant 0 \quad \text{if} \quad \begin{cases} 0 < \eta \leqslant \eta_{cr1} & \text{for} \quad 0 < \Omega \leqslant \Omega_{cr1} \\ 0 < \eta \leqslant 1 & \text{for} \quad \Omega_{cr1} < \Omega < f \end{cases} \tag{14}$$

$$\tilde{r}_{12} \geqslant 0 \quad \text{if} \quad 1 \leqslant \eta \leqslant \eta_{cr1} \quad \text{and} \quad 0 < \Omega \leqslant \Omega_{cr1} \tag{15}$$

where

$$\eta_{cr1} = \sqrt{1 + \left(\frac{p}{q}\right)^2} \geqslant 1 \tag{16}$$

$$\Omega_{cr1} = \sqrt{\frac{f^2 + 1 - \sqrt{(f^2 + 1)^2 - 4(1 - \mu_b)f^2}}{2(1 - \mu_b)}} \tag{17}$$

(iii) $\tilde{\beta} = \tilde{\theta} + \pi$. Substitution of $\tilde{\beta} = \tilde{\theta} + \pi$ into Eqs. (7.1) and (7.2) gives, after some rearrangements,

$$\begin{cases} -[(\Omega^2 - 1)\tilde{r} - \mu_b \tilde{\delta}\Omega^2] = \dfrac{\mu_b \Omega^2 \cos\tilde{\theta}}{\eta} \\ -2\zeta\Omega r = \dfrac{\mu_b \Omega^2 \sin\tilde{\theta}}{\eta} \end{cases}$$

Eliminating $\tilde{\theta}$, we obtain the two possible solutions as

$$\left.\begin{matrix} \tilde{r}_{21} \\ \tilde{r}_{22} \end{matrix}\right\} = R_{NS}(\eta \cdot p \pm \sqrt{D_{NS}}) \tag{18}$$

The corresponding $\tilde{\theta}$ and $\tilde{\delta}$ are determined by

$$\tilde{\theta} = \tan^{-1} \frac{2\varsigma\Omega \cdot \tilde{r}}{(\Omega^2 - 1) \cdot \tilde{r} - \mu_b \Omega^2 \tilde{\delta}} \tag{19}$$

$$\tilde{\delta} = 1 - \frac{\Omega^2 \tilde{r}}{f^2 - \Omega^2} \tag{20}$$

Note that $\tilde{\delta}$ may be negative even when $\tilde{r}$ is positive. Therefore, besides $\tilde{r} \geqslant 0$, we also need to derive the conditions for $\tilde{\delta} \geqslant 0$. The conditions under which $\tilde{r}_{21}$, $\tilde{r}_{22}$, and the associated $\tilde{\delta}$'s are non-negative are summarized as follows:

$$\tilde{r}_{21} \geqslant 0 \quad \text{and} \quad \tilde{\delta}_{21} \geqslant 0 \quad \text{if} \quad \begin{cases} \eta_{cr2} \leqslant \eta \leqslant 1 & \text{for} \quad 0 < \Omega \leqslant \Omega_{cr1} \\ \eta_{cr2} \leqslant \eta \leqslant \eta_{cr1} & \text{for} \quad \Omega_{cr1} < \Omega < 1 \quad \text{and} \quad P_{NS} \geqslant 0 \\ \eta_{cr2} \leqslant \eta \leqslant \eta_{cr1} & \text{for} \quad 1 \leqslant \Omega < f \end{cases} \tag{21}$$

$$\begin{cases} \tilde{r}_{22} \geqslant 0 \quad \text{and} \quad \tilde{\delta}_{22} \geqslant 0 \quad \text{if} \quad \begin{cases} 1 \leqslant \eta \leqslant \eta_{cr1} & \text{for} \quad \Omega_{cr1} < \Omega < 1 \quad \text{and} \quad P_{NS} > 0 \\ 1 \leqslant \eta < \eta_{cr2} & \text{for} \quad \Omega_{cr1} < \Omega < 1 \quad \text{and} \quad P_{NS} \leqslant 0 \\ 1 \leqslant \eta \leqslant \eta_{cr1} & \text{for} \quad 1 \leqslant \Omega < f \end{cases} \\ \tilde{r}_{22} \quad \text{does not exist for} \quad 0 < \Omega < \Omega_{cr1} \end{cases} \tag{22}$$

in which

$$P_{NS} = p(f^2 - \Omega^2)(\Omega^2 - 1) + q^2 \tag{23}$$

$$\eta_{cr2} = \frac{\Omega^4 \mu_b}{(f^2 - \Omega^2)\sqrt{(\Omega^2 - 1)^2 + 4\varsigma^2\Omega^2}} \tag{24}$$

Figure 2 is a typical plot of the regions of existence of the equilibrium positions on the $\eta - \Omega$ plane. The results indicate that at most two equilibrium positions may exist at a fixed rotational speed.

4 Stability

The behavior of a nonlinear system depends on the stability of the equilibrium positions. For an autonomous system, the stability of an equilibrium position can be determined by the eigenvalues of the associated linearized equations. To avoid the burden of determining the eigenvalues accurately, the Routh-Hurwitz criteria [13] are used to study the stability of each equilibrium position with the variations of some important system parameters.

Figure 3 shows the stable regions of the equilibrium positions on the $\zeta - \Omega$ plane for $\eta > 1$. In the triangular shaded area, no equilibrium positions exist. Although Fig. 2 indicates that, for a given value in the range $\eta > 1$, both $\tilde{r}_{11}$ and $\tilde{r}_{12}$ exist if the rotational speed is less than a critical value, only $\tilde{r}_{11}$ is stable. Simi-

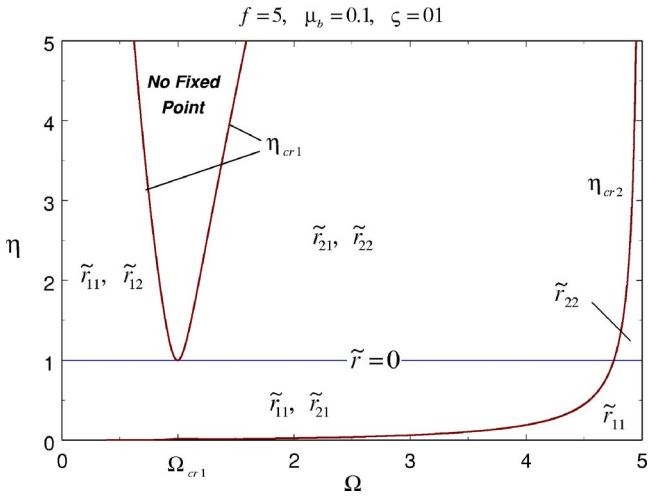

Fig. 2 Regions of existence of the equilibrium positions

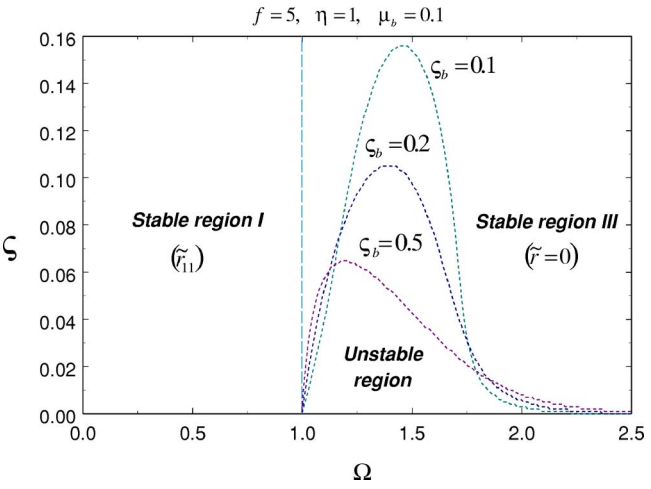

Fig. 4 Stability diagram on the $\zeta-\Omega$ plane for $\eta=1$

larly, although $\tilde{r}_{21}$ and $\tilde{r}_{22}$ both exist when the rotational speed is above a critical value, only $\tilde{r}_{22}$ is stable. In Fig. 3, the equilibrium position $\tilde{r}_{11}$ is stable between the vertical axis and the left boundary of the shaded area. The dashed lines to the right of the shaded area are the boundaries of the unstable region of $\tilde{r}_{22}$ for different values of ζ_b. For a given value of ζ_b, $\tilde{r}_{22}$ is unstable below the associated dashed line. For example, at point A ($\Omega=1.25$, $\zeta=0.1$), the equilibrium position $\tilde{r}_{22}$ is unstable for $\zeta_b=0.2$, but stable for $\zeta_b=0.5$.

Figure 4 shows the stable regions on the $\zeta-\Omega$ plane for $\eta=1$. The equilibrium position $\tilde{r}_{11}$ is stable for $\Omega<\Omega_{cr1}(\approx 1)$. For $\Omega>\Omega_{cr1}$, the only possible stable equilibrium position is the perfect balancing position, denoted by $\tilde{r}=0$. The dashed lines are the boundaries of the unstable regions of the perfect balancing position for different values of ζ_b. For a given value of ζ_b, the perfect balancing position is unstable in the area enclosed by the corresponding dashed line and the horizontal axis.

The stability diagram for $\eta<1$ is shown in Fig. 5. For $\eta<1$, as indicated by Fig. 2, two equilibrium positions, $\tilde{r}_{11}$ and $\tilde{r}_{21}$, exist. Among them, $\tilde{r}_{21}$ is always unstable; the only possible stable equilibrium position is $\tilde{r}_{11}$. In Fig. 5, the dashed lines are the boundaries of the unstable regions of $\tilde{r}_{11}$ for various values of ζ_b. Inside the area surrounded by the dashed line and the horizontal axis, $\tilde{r}_{11}$ is unstable.

Among all the equilibrium positions, the perfect balancing position is of the most practical interest. A balancer with a larger stable region of the perfect balancing position can tolerate a larger amount of variations in the system parameters. We thus proceed to study the effects of the additional degree of freedom in the radial direction on the stable region of the perfect balancing position. For the ball-rod-spring balancer, since the distance between the ball and the geometric center of the disk changes with the rotational speed, $\eta=1$ only at a particular value of Ω. In other words, perfect balancing can only be achieved at a particular rotational speed. Hence, we would like to study the stability of the perfect balancing position at a fixed rotational speed. Figure 6 shows the stable region of the perfect balancing position on the $\zeta-\zeta_b$ plane for different values of f. The dashed lines are the boundaries of the stable region for the specified values of f. The perfect balancing position is stable in the area above and to the right of the dashed line. As can be seen from Fig. 6, the stable region of the perfect balancing position increases as the value of f decreases. Note that f is the ratio of the natural frequency of the ball-rod-spring unit to that of the system. A large value of f, say $f=100$, indicates a very stiff radial spring. In this case, the radial displacement of the ball is negligible and the dashed line of $f=100$ approximates well to the boundary of the stable region of $\tilde{r}=0$ of the fixed-orbit balancer. Since the stable region of $f=6$ is relatively larger than that of $f=100$, we can conclude that introducing the

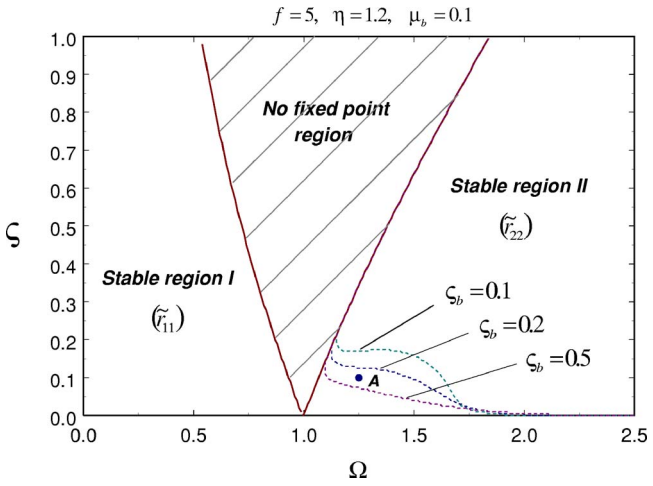

Fig. 3 Stability diagram on the $\zeta-\Omega$ plane for $\eta>1$

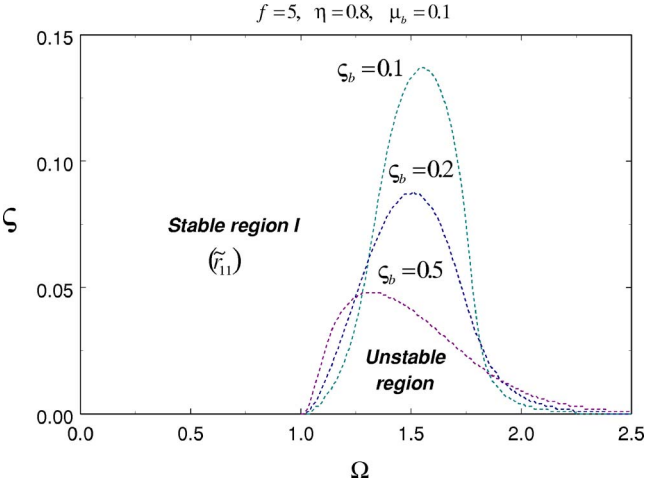

Fig. 5 Stability diagram on the $\zeta-\Omega$ plane for $\eta<1$

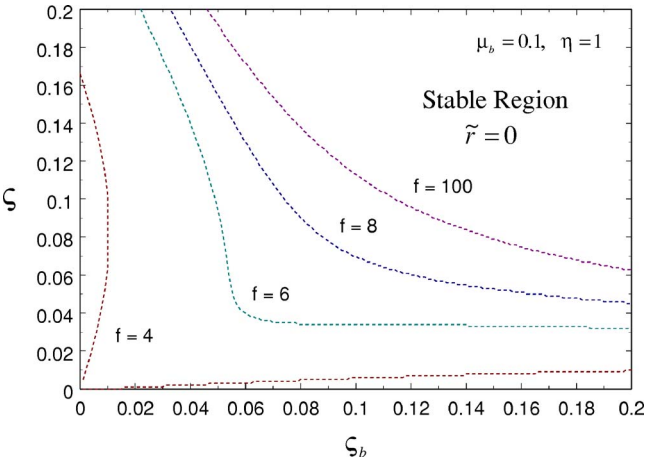

Fig. 6 Stable region of the perfect balancing position on the $\zeta_b - \zeta$ plane at a constant rotational speed for different values of f

radial degree of freedom may broaden the stable region of perfect balancing position if the design parameters are properly chosen.

5 Conclusion

This paper proposed a modified ball-type balancer that consists of several ball-rod-spring units rotating about the spindle freely. In the modified balancer, the ball cannot only move circumferentially around the spindle but also slide radially along the rod. The motion of the ball along the rod is restrained by a spring. The dynamic characteristics of the modified balancer with a single ball-rod-spring unit were investigated in detail, and closed-form formulas of the equilibrium positions were presented. The existence and stable regions of each equilibrium position in the parameter space were identified. It is found that there is, at most, one stable equilibrium position at a given rotational speed. The effects of the stiffness of the radial spring on the stable region of the perfect balancing position were examined. Numerical results indicate that the modified balancer may possess larger stable region of the perfect balancing position compared to the traditional fixed-orbit balancer. Since it takes at least two balls to suppress rotational vibrations due to arbitrary amount of imbalance, further study of the dynamic characteristics of the modified balancer with two ball-rod-spring units is required and is currently underway.

Acknowledgment

This work was supported by the National Science Council of R.O.C. under Grant No. NSC93-2212-E-002-066.

References

[1] Alexander, J. D., 1964, "An Automatic Dynamic Balancer," *Proc. for 2nd Southeastern Conference*, Vol. 2, pp. 415–426.
[2] Cade, J. W., 1965, "Self-Compensating Balancing in Rotating Mechanicsm," Des. News pp. 234–239.
[3] Bövik, P., and Högfors, C., 1986, "Autobalancing of Rotors," J. Sound Vib., **111**(3), pp. 429–440.
[4] Rajalingham, C., Bhat, R. B., and Rakheja, S., 1998, "Automatic Balancing of Flexible Vertical Rotors Using a Guided Ball," Int. J. Mech. Sci., **40**(9), pp. 825–834.
[5] Lee, J., and Moorhem, W. K. V., 1996, "Analytical and Experimental Analysis of a Self-Compensating Dynamic Balancer in a Rotating Mechanism," ASME J. Dyn. Syst., Meas., Control, **118**, pp. 468–475.
[6] Chung, J., and Ro, D. S., 1999, "Dynamic Analysis of An Automatic Dynamic Balancer for Rotating Mechanisms," J. Sound Vib., **228**(5), pp. 1035–1056.
[7] Kang, J.-R., Chao, C.-P., Huang, C.-L., and Sung, C.-K., 2001, "The Dynamics of a Ball-Type Balancer System Equipped With a Pair of Free-Moving Balancing Masses," ASME J. Vibr. Acoust., **123**, pp. 456–465.
[8] Hung, W.-Y., Chao, C.-P., Kang, J.-R., and Sung, C.-K., 2002, "The Application of Ball-Type Balancers for Radial Vibration Reduction of High-Speed Optic Disk Drives," J. Sound Vib., **250**, pp. 415–430.
[9] Yang, Q., Ong, E.-H., Sun, J., Guo, G., and Lim, S.-P., 2005, "Study on the Influence of Friction in an Automatic Ball Balancing System," J. Sound Vib., **285**, pp. 73–99.
[10] Chao, C.-P., Sung, C.-K., and Wang, C.-C., 2005, "Dynamic Analysis of the Optical Disk Drives Equipped With an Automatic Ball Balancer With Consideration of Torsional Motions," ASME J. Appl. Mech., **72**, pp. 826–842.
[11] Lu, C. J., 2006, "Stability Analysis of a Single-Ball Automatic Balancer," ASME J. Vibr. Acoust., **128**, pp. 122–125.
[12] Lu, C. J., 2005, "A Novel Design of Ball-Type Automatic Balancer," *Proc. of 1st International Symposium on Advanced Technology of Vibration and Sound*, Hiroshima, pp. 311–315.
[13] Ogata, K., 1970, *Modern Control Engineering*, Prentice-Hall, Englewood Cliffs NJ.